A Simple Method for Computing the Resonant Frequencies of Microstrip Ring Resonators

SOTIRIOS G. PINTZOS, MEMBER, IEEE, AND REINHOLD PREGLA, MEMBER, IEEE

Abstract—**A simple and efficient method for the computation of the resonant frequencies of microstrip ring resonators is presented. By means of the "reaction concept" a stationary formula for the resonant frequency of these resonators is derived. In this context a suitable approximation for the current distribution on the strip pertaining to the dominant mode has been made. The numerical results are in excellent agreement with experimental data corroborating the accuracy of the presented method.**

I. Introduction

Microstrip resonators of various forms have become indispensable elements of today's microwave integrated circuits. They are used either as single components, i.e., as frequency determining parts of oscillator circuits, or in coupled form for the realization of filters, couplers, and other microwave circuits. Their practical importance suggests the development of methods of analysis which, by making use of appropriate analytical and numerical means, lead to accurate results for relevant parameters. Up to date the analysis of microstrip resonators has been carried out either on the basis of simplified models of the real structure ("model of magnetic walls") [7], [8] or by imbedding the resonator in a closed waveguide to circumvent the intrinsic analytical difficulties of open waveguiding structures [4], [6]. The procedure first mentioned is, of course, of limited applicability, where the second can be numerically very expensive and, because of its very nature, cannot take into account the influence of radiation effects.

This paper deals with open microstrip ring resonators of which the resonant frequency will be determined. In the following, a relatively simple and numerically inexpensive nonetheless efficient method of analysis will be given based on the so-called stationary principle. This principle has been utilized successfully in the case of the straight microstripline [2]. Experimental data will be compared with the numerical results in order to test the accuracy of the present method.

Manuscript received October 19, 1977.

S. G. Pintzos is with the Institut für Hoch- und Höchstfrequenztechnik der Ruhr-Universität Bochum, D-4630 Bochum, Germany, POB 2148.

R. Pregla is with the Institut für Elektrotechnik, Fernuniversität, D-5800 Hagen, Germany, POB 940.

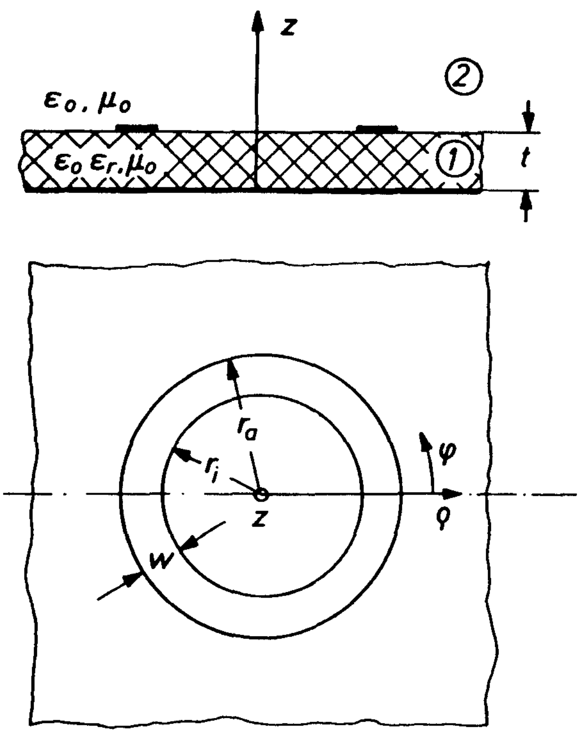

Fig. 1. Microstrip ring resonator with cylindrical coordinate system.

II. Method of Analysis

The structure under investigation is shown in Fig. 1. The substrate material is supposed to be linear, isotropic, and loss free. The strip and ground plate are ideal conductors. Further, it is assumed that the thickness of the strip is negligible. The method of analysis presented here is based on the variational or stationary principle. By means of the well-known "reaction concept" of electromagnetic theory [1], a stationary expression for the quantity to be determined, i.e., the resonant frequency for the dominant mode, will be established. The reaction of a field $\vec{E}^a, \vec{H}^a$ on a source $\vec{J}^b, \vec{M}^b$ in a volume V is defined as

$$\langle a,b\rangle = \int_V (\vec{E}^a \cdot \vec{J}^b - \vec{H}^a \cdot \vec{M}^b)\, dV. \tag{1}$$

In the case of a resonant structure, the self-reaction $\langle a,a\rangle$, the reaction of the field on its own source, is zero because the true field at resonance is source free. An approximate expression for the self-reaction can be de-

0018-9480/78/1000-0809$00.75 ©1978 IEEE

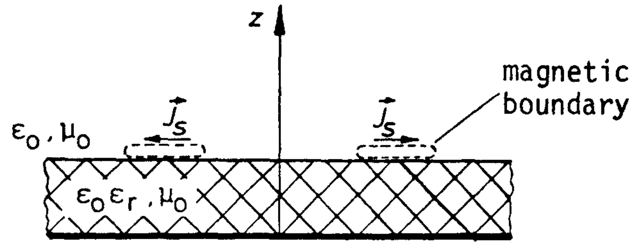

Fig. 2. Microstrip ring resonator with equivalent source.

rived using either a trial field or a trial source or both. It can be shown that by equating this expression to the correct reaction, a stationary formula for the resonant frequency of the structure under consideration can be obtained [9]. Now, according to the statements of both the uniqueness and equivalence theorems and in order to facilitate the formulation of our problem, the Huygens' source $\vec{J}_s = \vec{n} \times \vec{H}$ at the plane $z = t$ is introduced, as depicted in Fig. 2. In our case we are going to use a trial current distribution on the strip. Thus the field associated with such a current can be considered as a trial field as well. Hence, the starting point for our analysis is the expression

$$\langle a,a\rangle = \int_V \vec{E}_{tr}\cdot\vec{J}_{tr}\cdot dV = 0. \tag{2}$$

The index tr means "trial."

III. Field Representation

The field existing in the structure shown in Fig. 1 can be expressed in terms of two Cartesian vector potentials $\vec{A} = \vec{u}_z\Psi^E$ and $\vec{F} = \vec{u}_z\Psi^H$ by means of the following relations:

$$\vec{E} = -\text{rot}\,\vec{F} + \frac{1}{j\omega\epsilon_0\epsilon_r}\,\text{rot rot}\,\vec{A} \tag{3}$$

$$\vec{H} = \text{rot}\,\vec{A} + \frac{1}{j\omega\mu_0}\,\text{rot rot}\,\vec{F}. \tag{4}$$

The scalar potentials Ψ^E, Ψ^H satisfy the Helmholtz equation:

$$\Delta\Psi^E + k_i^2\Psi^E = 0 \tag{5a}$$

$$\Delta\Psi^H + k_i^2\Psi^H = 0 \tag{5b}$$

where

$$k_i^2 = k_0^2\epsilon_{ri} \tag{6}$$

and $i = 1,2$ designates the subregions 1 (substrate) and 2 (air), respectively. Δ is the Laplace operator in cylindrical coordinates and k_0 the wavenumber in vacuum. Assuming that the azimuthal dependence of the field is given by harmonic functions $h_\phi(n\phi)$ and taking into account that the geometry under consideration is infinite in radial direction, we represent the solution of (5) in the form of Fourier–Bessel integrals.

$$\Psi_i^E(\rho,\phi,z) = h_\phi^E(n\phi)\cdot\int_0^\infty \overline{\Psi}_{n,i}^E(k_\rho)\cdot k_\rho J_n(k_\rho\cdot\rho)\cdot h_{z,i}^E(\gamma_i z)\cdot dk_\rho \tag{7a}$$

$$\Psi_i^H(\rho,\phi,z) = h_\phi^H(n\phi)\cdot\int_0^\infty \overline{\Psi}_{n,i}^H(k_\rho)\cdot k_\rho J_n(k_\rho\cdot\rho)\cdot h_{z,i}^H(\gamma_i z)\cdot dk_\rho \tag{7b}$$

where

$$\gamma_i^2 + k_i^2 = k_\rho^2, \qquad i = 1,2 \tag{8a}$$

and $h_{z,i}(\gamma_i z)$ are harmonic functions expressing the z dependence of the field. They have to be chosen according to the boundary conditions to be satisfied at $z = 0$ and the radiation condition at $z \to +\infty$.

The potentials Ψ for the particular regions are to be formulated as follows.

In dielectric:

$$\Psi^E(\rho,\phi,z) = \sin(n\phi)\cdot\int_0^\infty A_n(k_\rho)\cdot\cosh(\gamma_1 z)\cdot k_\rho\cdot J_n(k_\rho\rho)\,dk_\rho \tag{8b}$$

$$\Psi^H(\rho,\phi,z) = \cos(n\phi)\int_0^\infty B_n(k_\rho)\sinh(\gamma_1 z)k_\rho J_n(k_\rho\rho)\,dk_\rho \tag{8c}$$

$$\gamma_1^2 + k_0^2\epsilon_r = k_\rho^2. \tag{9}$$

In air:

$$\Psi^E(\rho,\phi,z) = \sin(n\phi)\int_0^\infty C_n(k\rho)e^{-\gamma_2(z-t)}k_\rho J_n(k_\rho\rho)\,dk_\rho \tag{10a}$$

$$\Psi^H(\rho,\phi,z) = \cos(n\phi)\int_0^\infty D_n(k_\rho)e^{-\gamma_2(z-t)}k_\rho J_n(k_\rho\rho)\,dk_\rho \tag{10b}$$

$$\gamma_2^2 + k_0^2 = k_\rho^2. \tag{11}$$

The next step is to derive the field components needed for the formulation of the boundary conditions at the interface $z = t$. These conditions yield the equations necessary for determining the coefficients A_n, B_n, C_n, D_n in terms of the current distribution at $z = t$. The continuity conditions at the interface $z = t$ are as follows:

$$E_{\rho,1} = E_{\rho,2} \tag{12a}$$

$$E_{\phi,1} = E_{\phi,2} \tag{12b}$$

$$H_{\rho,1} - H_{\rho,2} = -I_\phi(\rho,\phi) \tag{13a}$$

$$H_{\phi,1} - H_{\phi,2} = I_\rho(\rho,\phi) \tag{13b}$$

where $I_\rho(\rho,\phi)$ and $I_\phi(\rho,\phi)$ are the components of the sheet current density $\vec{J}_s$ in ρ and ϕ direction, respectively.

The field components derived from (8) and (10) by means of (3) and (4) are now inserted in (12) and (13). This leads to a system of equations in the ρ domain. In order to obtain the final system for the unknowns A_n, B_n, C_n, D_n they have to be transformed into the k_ρ domain by means of the Hankel transform. This task can be facilitated by first unifying the order of the Bessel functions under the integral sign. Appropriate rearrangement of the ρ-domain equations and application of the recurrence relations for Bessel functions leads to the equations given in the Appendix. Hankel-transforming these equations and making use of the orthogonality relationship

$$\int_0^\infty J_\nu(k_\rho\rho)J_\nu(k'_\rho\rho)\rho d\rho = \frac{1}{\sqrt{k_\rho k'_\rho}}\delta(k_\rho - k'_\rho) \quad (14)$$

we arrive finally at the following system of linear equations for A_n, B_n, C_n, D_n:

$$\begin{bmatrix} \gamma_1 \sinh(\gamma_1 t) & j\omega\epsilon_0\epsilon_r \sinh(\gamma_1 t) & \gamma_2\epsilon_r & -j\omega\epsilon_0\epsilon_r \\ \gamma_1 \sinh(\gamma_1 t) & -j\omega\epsilon_0\epsilon_r \sinh(\gamma_1 t) & \gamma_2\epsilon_r & j\omega\epsilon_0\epsilon_r \\ -k_\rho \cosh(\gamma_1 t) & -\frac{\gamma_1 k_\rho \cosh(\gamma_1 t)}{j\omega\mu_0} & k_\rho & -\frac{\gamma_2 k_\rho}{j\omega\mu_0} \\ k_\rho \cosh(\gamma_1 t) & -\frac{\gamma_1 k_\rho \cosh(\gamma_1 t)}{j\omega\mu_0} & -k_\rho & -\frac{\gamma_2 k_\rho}{j\omega\mu_0} \end{bmatrix} \cdot \begin{bmatrix} A_n(k_\rho) \\ B_n(k_\rho) \\ C_n(k_\rho) \\ D_n(k_\rho) \end{bmatrix} = \begin{bmatrix} 0 \\ 0 \\ \bar{I}_{\rho,n-1} + \bar{I}_{\phi,n-1} \\ \bar{I}_{\rho,n+1} - \bar{I}_{\phi,n+1} \end{bmatrix} \quad (15)$$

where

$$\bar{I}_{\phi,n\pm1}(k_\rho) = \int_0^\infty I_\phi(\rho)\rho J_{n\pm1}(k_\rho\rho)\,d\rho \quad (16)$$

$$\bar{I}_{\rho,n\pm1}(k_\rho) = \int_0^\infty I_\rho(\rho)\rho J_{n\pm1}(k_\rho\rho)\,d\rho \quad (17)$$

are the Hankel transforms of order $n \pm 1$ of the ρ-dependent parts of the sheet current components $I_\phi(\rho,\phi)$ and $I_\rho(\rho,\phi)$, respectively.

The solution of (15) is as follows:

$$A_n(k_\rho) = -\frac{1}{2}\frac{\gamma_2\epsilon_r}{k_0}\frac{\bar{I}_{n-1} - \bar{I}_{n+1}}{\cosh(\gamma_1 t)(\gamma_2/k_0\,\epsilon_r + \gamma_1/k_0 \tanh(\gamma_1 t))} \quad (18a)$$

$$B_n(k_\rho) = -\frac{j}{2}\frac{k_0}{\omega\epsilon_0}\frac{\bar{I}_{n-1} + \bar{I}_{n+1}}{\sinh(\gamma_1 t)(\gamma_2/k_0 + \gamma_1/k_0 \coth(\gamma_1 t))} \quad (18b)$$

$$C_n(k_\rho) = \frac{1}{2}\frac{\gamma_1}{k_0}\frac{(\bar{I}_{n-1} - \bar{I}_{n+1})\tanh(\gamma_1 t)}{(\gamma_2/k_0\,\epsilon_r + \gamma_1/k_0 \tanh(\gamma_1 t))} \quad (18c)$$

$$D_n(k_\rho) = -\frac{j}{2}\frac{k_0}{\omega\epsilon_0}\frac{\bar{I}_{n-1} + \bar{I}_{n+1}}{(\gamma_2/k_0 + \gamma_1/k_0 \coth(\gamma_1 t))} \quad (18d)$$

where

$$\bar{I}_{n-1} \mp \bar{I}_{n+1} = k_\rho^{-1}\{(\bar{I}_{\phi,n-1} \pm \bar{I}_{\phi,n+1}) + (\bar{I}_{\rho,n-1} \mp \bar{I}_{\rho,n+1})\}. \quad (19)$$

III. The Stationary Expression for the Resonant Frequency

After having expressed the coefficients A_n, B_n, C_n, and D_n in terms of the Hankel-transformed current distribution at the interface $z = t$, we now proceed to derive the stationary formula for the eigenvalue of the resonant structure under consideration starting from (2). Carrying out the integration over ϕ and z, the integral in (2) becomes

$$\int_0^\infty [E_{\phi,i}(\rho, z=t)I_\phi(\rho) + E_{\rho,i}(\rho, z=t)I_\rho(\rho)]\rho\,d\rho = 0 \quad (20)$$

where $i = 1$ or 2.

In the following we shall neglect the ρ component of the current on the grounds that in the case of the microstripline the transverse component of current is essentially smaller than the longitudinal component. Because the ring resonator can be thought of as a line resonator bent to a ring, this result is surely applicable to the ring resonator on the condition that the ratio w/r_i does not become very large. Finally we have

$$\int_0^\infty E_{\phi,i}(\rho, z=t)I_\phi(\rho)\rho\,d\rho = 0. \quad (21)$$

Now the ϕ-independent part of $E_{\phi,i}$ is evaluated at $z = t$ and inserted in (21). Assuming the validity of interchanging the order of integration and recalling the definition of Hankel transformation we then obtain

$$\int_0^\infty \left[\frac{\gamma_1\gamma_2 \tanh(\gamma_1 t)(\bar{I}_{\phi,n-1} + \bar{I}_{\phi,n+1})^2}{\gamma_2\epsilon_r + \gamma_1 \tanh(\gamma_1 t)} - k_0^2\frac{(\bar{I}_{\phi,n-1} - \bar{I}_{\phi,n+1})^2}{\gamma_2 + \gamma_1 \coth(\gamma_1 t)}\right] k_\rho \cdot dk_\rho = 0. \quad (22)$$

This simple formula is the characteristic equation for the eigenvalue k_0 (i.e., the resonant frequency). A similar formula has been derived for straight microstrips [3]. k_0 is, of course, a complex quantity because of radiation losses which are inherent to open resonant structures. Here we are only interested in the real part of this quantity. As far as the integration contour in the complex k_ρ plane is concerned, the real axis has been chosen as a matter of convenience. The choice of the sign of the two-valued function $\gamma_2 = \sqrt{k_\rho^2 - k_0^2}$ must comply with the requirements of the radiation condition.

IV. Choice of Current Distribution and Numerical Results

The criteria underlying the choice of the trial current distribution may now be discussed. In the case of the microstripline the approximation of the current distribution (longitudinal component) by the function which describes the static charge distribution on the strip has proven to be an appropriate choice [2]. Now evoking the resemblance of current distribution for the dominant mode of the microstripline and ring resonator, we adequately may approximate the current distribution at $z = t$ (Fig. 1) by the following expression:

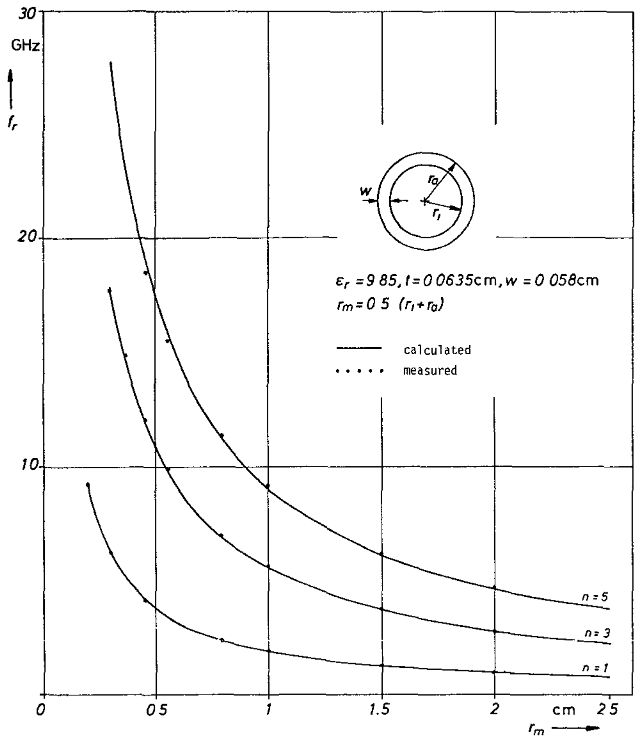

Fig. 3. Resonant frequency of microstrip ring resonator versus the mean radius r_m. n is the azimuthal resonance order.

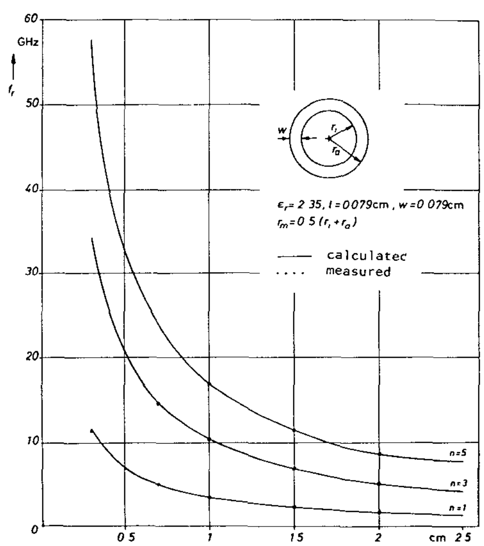

Fig. 4. Resonant frequency of microstrip ring resonator versus the mean radius r_m. n is the azimuthal resonance order.

$$I_\phi(\rho) = \frac{\text{const.}}{\sqrt{1-\left[\frac{2(\rho-r_m)}{w}\right]^2}} \tag{23}$$

where

$$r_m = \tfrac{1}{2}(r_i + r_a). \tag{24}$$

Unfortunately, there does not exist the Hankel transform of this function in the form of an analytical expression. Thus the integration required to obtain $\bar{I}_{\phi,\nu}(k_\rho)$ has to be performed numerically, essentially increasing the computational effort. The very good agreement of results obtained by using the approximation in (23) with results

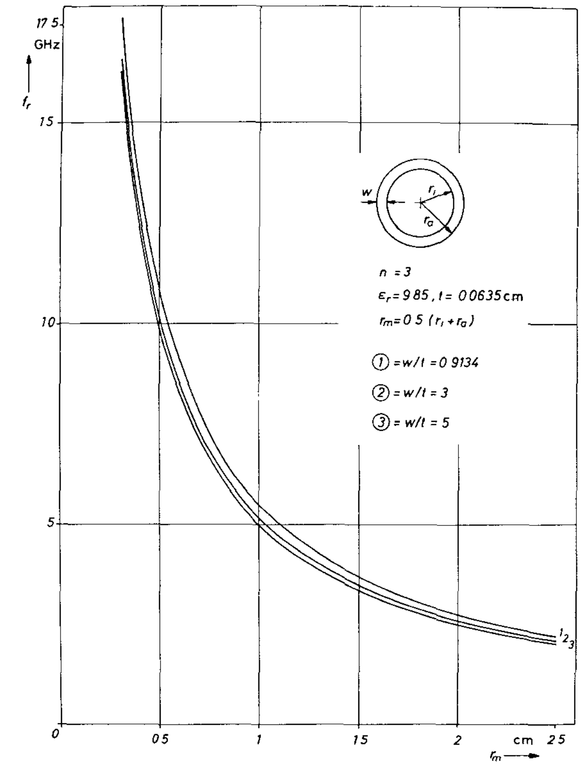

Fig. 5. Resonant frequency characteristic of microstrip resonator for different values of the structural parameter w/t.

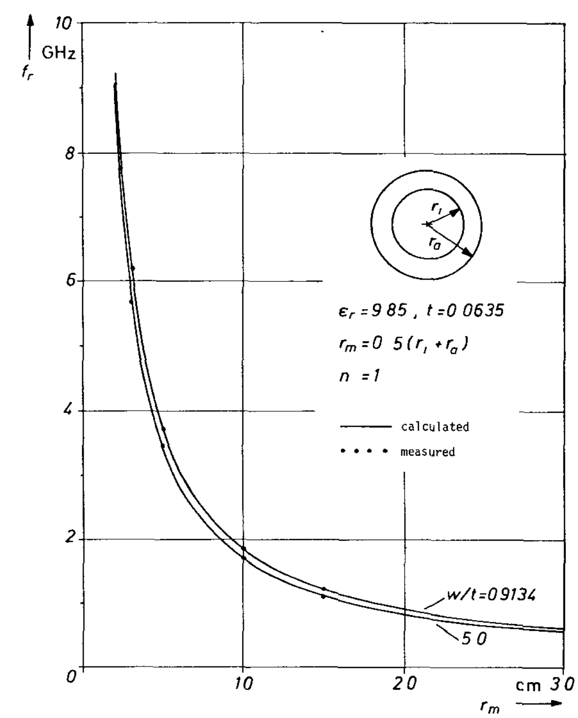

Fig. 6. Resonant frequency characteristic of microstrip ring resonator. n is the azimuthal resonance order.

arrived at using a constant distribution, at least for not very wide strips, finally led to the choice of the latter for our calculations, taking into account that in this case the Hankel transform can be given directly. The adequateness of this choice can be demonstrated by the very good agreement of calculated and measured results, as shown in Figs. 3, 4, and 6. The solution of (22) is obtained using a simple iterative method (*regula falsi*). To numerically evaluate the improper integral (22) an appropriate upper integration limit has to be determined. Taking into account that the integrand asymptotically decays as $0(k_\rho^{-3})$, values for the upper integration limit have been chosen according to this behavior.

The measurements have been performed using reflexion type resonators. The width of the coupling gap was $0,1,\cdots,0,4$ mm. The materials used for the measurements are Al_2O_3 with $\epsilon_r=9.85$ and Duroid with $\epsilon_r=2.35$. Their dielectric constants were measured according to the method given in [12].

V. Conclusion

A simple and accurate method based on the stationary principle is given for the computation of the resonant frequencies of microstrip ring resonators. Although crude approximations of the current distribution can be made, the numerical results are in excellent agreement with the experimental data. Because of the numerical inexpensiveness of this method reliable design charts for relevant parameters can be quickly established. It is obvious that (20) transformed into the k_ρ domain can also be used to compute the resonant frequency of microstrip disc resonators provided that suitable approximations for the current components in azimuthal and radial direction can be made.

Appendix

$$\frac{1}{j\omega\epsilon_0\epsilon_r}\int_0^\infty A_n(k_\rho)\cdot\gamma_1\cdot\sinh(\gamma_1 t)\cdot J_{n-1}(k_\rho\cdot\rho)\cdot dk_\rho + \int_0^\infty B_n(k_\rho)\cdot k_\rho^2\cdot\sinh(\gamma_1 t)\cdot J_{n-1}(k_\rho\cdot\rho)\cdot dk_\rho = -\frac{1}{j\omega\epsilon_0}\cdot\int_0^\infty C_n(k_\rho)\cdot\gamma_2\cdot k_\rho^2\cdot J_{n-1}(k_\rho\cdot\rho)\cdot dk_\rho + \int_0^\infty D_n(k_\rho)\cdot k_\rho^2\cdot J_{n-1}(k_\rho\cdot\rho)\cdot dk_\rho. \tag{A1}$$

$$\frac{1}{j\omega\epsilon_0\epsilon_r}\cdot\int_0^\infty A_n(k_\rho)\cdot\gamma_1\cdot\sinh(\gamma_1 t)\cdot k_\rho^2\cdot J_{n+1}(k_\rho\cdot\rho)\cdot dk_\rho - \int_0^\infty B_n(k_\rho)\cdot\sinh(\gamma_1 t)\cdot k_\rho^2\cdot J_{n+1}(k_\rho\cdot\rho)\cdot dk_\rho = -\frac{1}{j\omega\epsilon_0}\cdot\int_0^\infty C_n(k_\rho)\cdot\gamma_2\cdot k_\rho^2\cdot J_{n+1}(k_\rho\cdot\rho)\cdot dk_\rho - \int_0^\infty D_n(k_\rho)\cdot k_\rho^2\cdot J_{n+1}(k_\rho\cdot\rho)\cdot dk_\rho. \tag{A2}$$

$$-\int_0^\infty A_n(k_\rho)\cdot\cosh(\gamma_1 t)\cdot k_\rho^2\cdot J_{n-1}(k_\rho\cdot\rho)\cdot dk_\rho - \frac{1}{j\omega\mu_0}\cdot\int_0^\infty B_n(k_\rho)\cdot\gamma_2\cdot\cosh(\gamma_1 t)\cdot k_\rho^2\cdot J_{n-1}(k_\rho\cdot\rho)\cdot dk_\rho + \int_0^\infty C_n(k_\rho)\cdot k_\rho^2\cdot J_{n-1}(k_\rho\cdot\rho)\cdot dk_\rho - \frac{1}{j\omega\mu_0}\cdot\int_0^\infty D_n(k_\rho)\cdot\gamma_2\cdot k_\rho^2\cdot J_{n-1}(k_\rho\cdot\rho)\cdot dk_\rho = I_\rho(\rho)+I_\phi(\rho). \tag{A3}$$

$$\int_0^\infty A_n(k_\rho)\cdot\cosh(\gamma_1 t)\cdot k_\rho^2\cdot J_{n+1}(k_\rho\cdot\rho)\cdot dk_\rho - \frac{1}{j\omega\mu_0}\cdot\int_0^\infty B_n(k_\rho)\cdot\gamma_1\cosh(\delta_1 t)\cdot k_\rho^2\cdot J_{n+1}(k_\rho\cdot\rho)\cdot dk_\rho - \int_0^\infty C_n(k_\rho)\cdot k_\rho^2\cdot J_{n+1}(k_\rho\cdot\rho)\cdot dk_\rho - \frac{1}{j\omega\mu_0}\cdot\int_0^\infty D_n(k_\rho)\cdot\gamma_2\cdot k_\rho^2\cdot J_{n+1}(k_\rho\cdot\rho)\cdot dk_\rho = I_\rho(\rho)-I_\phi(\rho). \tag{A4}$$

References

[1] V. H. Rumsey, "The reaction concept in electromagnetic theory," *Phys. Rev.*, ser. 2, vol. 94, no. 6, pp. 1483–1491, June 15, 1954.

[2] G. Kowalski and R. Pregla, "Dispersion characteristics of single and coupled microstrips," *Arch. Elek. Übertragung*, vol. 26, no. 6, pp. 276–280, 1972.

[3] R. Pregla and G. Kowalski, "Simple formulas for the determination of the characteristic constants of microstrips," *Arch. Elek. Übertragung*, vol. 28, no. 7/8, pp. 339–340, July 1974.

[4] T. Itoh, "Analysis of microstrip resonators," *IEEE Trans. Microwave Theory Tech.*, vol. MTT-22, pp. 946–951, Nov. 1974.

[5] T. Itoh and R. Mittra, "Analysis of a microstrip disc resonator," *Arch. Elek. Übertragung*, vol. 27, no. 11, pp. 456–458.

[6] R. Jansen, "Zur numerischen Berechnung geschirmter Streifenleitungsstrukturen," *Arch. Elek. Übertragung*, vol. 29, no. 6, pp. 241–247, June 1975.

[7] I. Wolff and N. Knoppik, "The microstrip ring resonator and dispersion measurements on microstrip lines," *Electron. Lett.*, vol. 7, pp. 779–781, Dec. 1971.

[8] Y. S. Wu and F. J. Rosenbaum, "Mode chart for microstrip ring resonators," *IEEE Trans. Microwave Theory Tech.*, vol. MTT-21, pp. 487–489, July 1973.

[9] R. Harrington, *Time-Harmonic Electromagnetic Fields*. New York: McGraw-Hill, 1961.

[10] I. N. Sneddon, *The Use of Integral Transforms*. New Delhi: Tata McGraw-Hill, 1974.

[11] Erdelyi *et al.*, *Tables of Integral Transforms*. New York: McGraw-Hill, 1954.

[12] J. Q. Howell, "A quick accurate method to measure the dielectric constant of MIC substrates," *IEEE Trans. Microwave Theory Tech.*, vol. MTT-21, pp. 142–143, Mar. 1973.